NOTES AND CORRESPONDENCE

Lagrangian Analysis and Predictability of Coastal and Ocean Dynamics 2000

ARTHUR J. MARIANO

University of Miami, Miami, Florida

ANNALISA GRIFFA

University of Miami, Miami, Florida, and Consiglio Nazionale (CNR)/IOF, La Spezia, Italy

TAMAY M. ÖZGÖKMEN

University of Miami, Miami, Florida

ENRICO ZAMBIANCHI

Instituto Universitario Navale, Naples, Italy

24 October 2001 and 2 February 2002

ABSTRACT

The first Lagrangian Analysis and Predictability of Coastal and Ocean Dynamics (LAPCOD) meeting took place in Ischia, Italy, 2–6 October 2000. The material presented at LAPCOD 2000 indicated both a maturing of Lagrangian-based observing systems and the development of new analysis and assimilation techniques for Lagrangian data. This summary presents a review of the state-of-the-art technology in Lagrangian exploration of oceanic and coastal waters that was presented at the meeting.

1. Introduction

It is an exciting time for the study of fluid motion from a Lagrangian perspective because of maturing observational techniques, new sensor technology and analysis methods, and increased computational power for numerical simulations. Multidisciplinary research involving biologists, physical oceanographers, mathematicians, and engineers is synergistically improving our understanding of chaotic advection, turbulent mixing, and nonlinear particle dynamics in biological and physical systems. In order to further accelerate this research, the first Lagrangian Analysis and Predictability of Coastal and Ocean Dynamics (LAPCOD) meeting took place in Ischia, Italy, from 2 to 6 October 2000 (see www.rsmas.miami.edu/LAPCOD). This paper is a review of the observational and theoretical results from LAPCOD 2000, as well as a summary of recommendations for future Lagrangian-based exploration of the biology and physics of oceanic and coastal waters.

Corresponding author address: Dr. Arthur J. Mariano, Rosenstiel School of Marine and Atmospheric Science, University of Miami, 4600 Rickenbacker Causeway, Miami, FL 33149-1098.
E-mail: amariano@rsmas.miami.edu

2. Observational results

Lagrangian data are primarily used by oceanographers for estimation of the climatological mean flow of the ocean and its marginal seas, and for the information that such data can provide on the basic statistics of subgrid-scale velocity and dispersion. New datasets span a vast range of geographical locations, instrument design [e.g., subsurface floats, different types of surface drifters, and high-frequency (HF) radar], and phenomena from basin-scale (important for climatic studies) to small-scale coastal observations targeted for environmental applications. Results for (near) surface circulation in the tropical Pacific, in the Caribbean, and in two subbasins of the Mediterranean Sea, the Adriatic Sea, and Balearic Sea, are presented next, followed by observations from subsurface RAFOS [sound transmission direction opposite to that of Sound Fixing and Ranging (SOFAR) technology] floats in the northeast Atlantic Ocean.

A new methodology for mean-flow eddy decomposition (Bauer et al. 1998) was used to estimate seasonal maps of eddy diffusivity from near-surface buoys in the tropical Pacific. Time-dependent mean flows are esti-

mated by fitting, for each horizontal velocity component, a least squares smoothing bi-cubic spline to bimonthly groupings of the data. The resulting residual mesoscale velocity is modeled as an autoregressive (AR) process (see below), and diffusivity estimates are derived from the parameters of an AR model. Zonal diffusivity estimates, 5–76 $\times$ 10^7 cm^2 s^{-1}, are, in general, larger than meridional estimates, 2–9 $\times$ 10^7 cm^2 s^{-1}. Larger values are found in regions of strong meridional shear between the North Equatorial Current (NEC) and the North Equatorial Countercurrent. Autoregressive models of order 1 (2) are appropriate for all zonal velocities and for weak (strong) meridional velocities. Lagrangian integral timescales are on the order of 2–3 days.

Seasonal maps of mean velocity in the Adriatic Sea, calculated from over 200 satellite-tracked drifters from 1990 to 1999, show three distinct recirculation cells in the northern, central, and southern subbasins (Poulain 1999, 2001). Mean velocities in the cyclonic gyres can exceed 25 cm s^{-1}, with maximum velocity variances exceeding 500 cm^2 s^{-2}. Along-isobath diffusivity is 2 $\times$ 10^7 cm^2 s^{-1}, with integral space scales and timescales of 18 km and 2 days, respectively. Cross-isobath diffusivity and spatiotemporal scales are approximately one-half of along-isobath estimates. Plots of mean kinetic energy and eddy kinetic energy vary as a function of the bin size used to calculate the mean flow and the autocovariance function, a result widely reported by others. A bin size in which both of these quantities saturate and are robust is required for good estimates of Lagrangian velocity statistics. Poulain (2001) used overlapping 40-km circular bins.

Approximately 100 near-surface buoys were launched in the Caribbean Sea during the last few years as part of the National Ocean Partnership Program (NOPP) ''Year of the Ocean'' project (Wilson and Leaman 2001). There is a broad westward flow in the northern and eastern parts of the Caribbean Basin, and a considerable number of both cyclonic and anticyclonic eddies exist. The flow in the southwest Caribbean is dominated by the quasi-permanent gyre known as the Panama–Colombia gyre. Drifters launched in this gyre have retention times of a few months, and one preferential pathway ends in the shelf waters off southern Cuba.

Bower et al. (2002) reviewed results of 44 RAFOS float trajectories at 1000-m depth near and offshore of the Iberian Peninsula. The float trajectories revealed four meddies near Cape Saint-Vincent, implying a formation rate of 15–20 meddies per year. Meddies, or Mediterrean eddies, named because their core consists of high-salinity water of Mediterrean Sea origin, are anticyclonic mesoscale eddies that take 3–7 days to form, have a velocity integral timescale of 3–4 days, and influence the path of the Mediterrean Undercurrent. The mean background flow was 15–20 cm s^{-1}, with peak velocities of 40 cm s^{-1}. On the other side of the Iberian Peninsula, in the northwestern Mediterranean, near-surface float observations in the Catalan Current in June 2000 measured a 30–40 cm s^{-1} flow. The Catalan Current primarily flows along the continental topography as it advects low-salinity water and fish larvae from the Gulf of Lions to the open sea (Sabatis et al. 2001). The floats also exhibited strong inertial oscillations after the passage of a storm.

Bezerra et al. (1998) used velocity measurements from buoys and video imaging techniques to estimate dispersion in the coastal waters of Spain and Brazil as a function of wind stress, wave height, strength of tidal currents, and distance from shore. Milk was used as the tracer for the imaging techniques. Horizontal diffusivity values ranged from 1 to 2 $\times$ 10^4 cm^2 s^{-1} and were a strong function of the wave Reynolds number and the wind stress. Anisotropy increased near the coast, presumably due to the alongshore currents.

One hundred fifteen isopycnal (σ_θ = 27.5) RAFOS floats were deployed by Rossby and colleagues in the subpolar fronts in two primary regions: just west of the Mid-Atlantic Ridge and along the eastern margin of the North Atlantic. These float trajectories appear to have preferred pathways, indicating a strong influence from topography, especially when stratification is weak and submesoscale/mesoscale mixing is strong. The mean flow is eastward through the Charlie Gibbs Fracture Zone, and there are two primary northward pathways: (i) northeast into the northern Iceland Basin west of the Rockall/Hatton Bank, then southwest along the Reykjanes Ridge, and then northward into the Irminger Sea; and (ii) abruptly to the northwest toward the Reykjanes Ridge.

Zhang et al. (2001) calculated an average Lagrangian integral timescale of 2 days for RAFOS floats in the North Atlantic Current and 3.2 days for floats in the Newfoundland Basin. These floats nominally sampled σ_θ 27.2 and 27.5 surfaces. Diffusivity values ranged from 1 to 7 $\times$ 10^7 cm^2 s^{-1} and space scales ranged from 20 to 30 km. These estimates are sensitive to the horizontal bin size used for calculating the mean flow and autocovariance functions. Since observations from over 100 floats were available, 1/2° $\times$ 1/2° horizontal bins had sufficient data to resolve the heterogeneous flow field with large mean velocity shear.

Residual velocity statistics for these floats, calculated by removing the arithmetic averages in the corresponding 1/2° $\times$ 1/2° bin from each float velocity, are approximately Gaussian only after the mean velocity shear is properly removed. Other methods for calculating mean velocity fields from Lagrangian data that are, in general, space and time-dependent, are discussed in Bauer et al. (1998) and Poulain (2001). The dispersion of the residual velocities follows Taylor's (1921) well-known result; that is, diffusivity grows linearly with time initially after launch, and, for a long time, it is proportional to the Lagrangian integral timescale T_L (the velocity variance is the constant in both cases). RAFOS floats have integral timescales on the order of 1 day

when isopycnals shoal, and deeper subtropical floats have timescales as long as 11.5 days. For comparison, SOFAR floats in the main and lower thermocline of the North Atlantic have timescales on the order of 1–2 weeks (Rossby et al. 1983).

Very interesting results for the surface circulation in limited domains can be obtained by combining Eulerian data with Lagrangian analysis. Results from high horizontal and temporal (250 m and 20 min) resolution ocean surface current radar (OSCR) surface velocity data from the 4D current experiment in the coastal region off Hollywood, Florida, during the summer of 1999 indicate significant dynamical events, including submesoscale vortices, large lateral meandering of the Florida Current on timescales of hours, eddy mergers, and periods of strong anomalous southward flow. Dominant periods are 27 h (inertial), 10 h (associated with a vorticity wave), and a few days (Florida Current meandering). Dominant spatial scales of the eddies are on the order of 2–3 km, with peak propagation speeds of 30–40 cm s^{-1} northward (Shay et al. 2000; Peters et al. 2002). Simulated trajectories ''launched'' at the latitude of the Broward County Sewage Outfall suggested that beaching of particles became more evident for particles launched within 2 km of the coast, and that most particles launched 4 km or more offshore exited the area.

Results from HF radar maps of surface currents in Monterey Bay reveal a flow field that consists of background and geostrophic currents, upwelling-induced currents, and sea-breeze-driven and tidal currents. These velocity data are used to simulate particle trajectories and are inputted to a dynamical system analysis. Both simulated particle trajectories and the dynamical system analysis indicate two distinct regimes for residence times of nearshore particles.

High-frequency velocity data can be projected onto geometrical orthogonal functions (GOFs) that consist of a vorticity basis (equal to streamfunction for zero divergence) and a divergence basis that is like the velocity potential (Lipphardt et al. 2000). Spectra of the modes reveal peaks at 1 and 2 cpd as a result of tides and wind forcing. Significant low-frequency energy also exists in vorticity modes associated with large-scale transport.

Inspection of trajectories from the Lagrangian data archives reveals that the descriptive character of Lagrangian trajectories in the ocean exhibits classical examples of both standard and nonstandard dispersion behaviors, most likely determined by the joint effects of turbulent diffusion and chaotic advection. A number of float clusters have either remained coherent for thousands of kilometers and many months, or dispersed rapidly and sampled vastly different parts of the oceans, even though they were launched ''close'' together. There are also trajectories from floats that were launched far apart and then almost *touched* each other, as well as float trajectories that are textbook examples of time-averaged general circulation of the ocean and of potential vorticity conservation (see Figs. 1 and 2; Rossby et al. 1983; Mariano and Rossby 1989; Garfield et al. 2001).

3. Biological studies

The Lagrangian approach is not widespread in the biological oceanographic community, even though it is probably the most natural one, since the motion of organisms in many cases can be considered at least partly coincident with the Lagrangian circulation. One of the reasons for this may well lie in the fact that the forcing results from the combination of biological and dynamical phenomena, and this often calls for the implementation of hybrid description and simulation techniques, that is, partly Lagrangian and partly Eulerian, which bring strong conceptual and technical difficulties. There are great possibilities for this approach, anticipated in the recent works by Hitchcock et al. (1997), Ye and Garvine (1998), Polivina et al. (1999), and Wolanski et al. (1997). There is also room for further improvement. Transport and dispersion of fish larvae and phytoplankton, for example, are especially well-suited for a Lagrangian-based analysis.

There is a debate about the degree of teleconnection between remote populations of fish in the Caribbean Sea. A key component needed to settle this debate is the dispersion rate of the fish larvae in the open sea and near the coast. Early models based on mean-flow advection and eddy dispersion, as well as genetic evidence, suggest that long-distance dispersal of larvae is likely a common event leading to considerable teleconnections among distant populations. However, new results (Cowen et al. 2000) demonstrate that local retention is more the rule and that long distance transport is likely insufficient, due to mortality, to sustain marine populations ecologically. Numerical model simulations and in situ data near Barbados support the hypothesis that coral fish larvae capitalize on flow structure to be retained in the proximity of their native island. Behavorial aspects of marine populations must also be modeled as close to reality as possible.

Numerical investigations of the vertical distribution of phytoplankton require simulating the behavior of phytoplankton cells using a biological model coupled to an advection–diffusion transport model. Results have been presented by Cianelli et al. (2001, manuscript submitted to *Antarct. Sci.*) for a one-dimensional Lagrangian model for the motion and growth of phytoplankton organisms, including mixed layer vertical velocities and turbulent eddy dispersion, a time- and depth-dependent light source for cell growth, self-shading effect, and nonlinear functions for growth/irradiance, photoinhibition, and photoadaptation processes. The combined influence of the different physical and biological factors on phytoplankton growth leads to nontrivial results, highlighting the strong importance of photoinhibition, with possible consequences in terms of optimization of

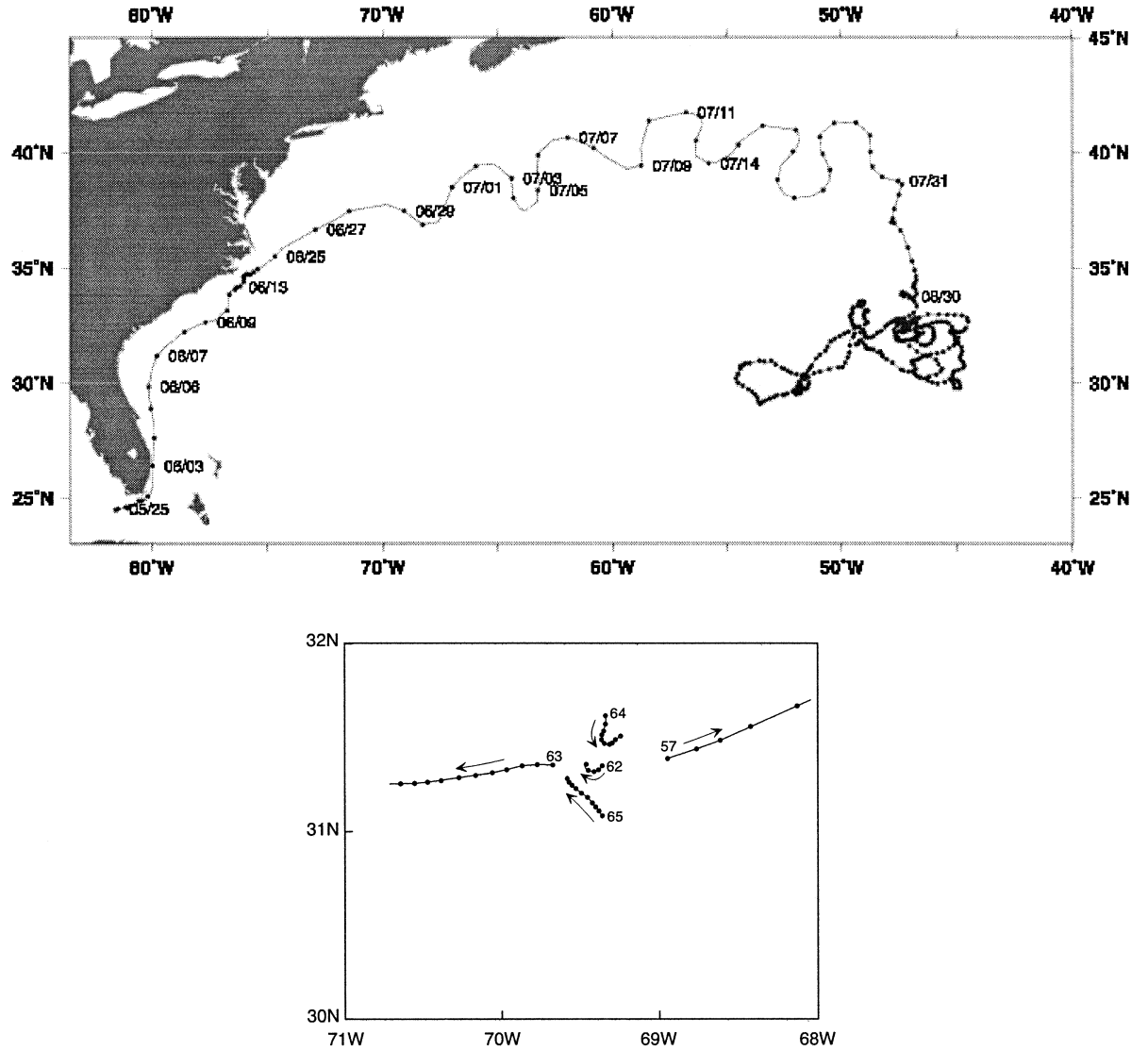

FIG. 1. (a) The trajectory of a holey-sock drifter drogued at 10-m depth. Launched off the Florida Keys by Tom Lee 25 May 1991, the drifter is entrained by the Florida Current, its path is deflected by the Charleston Bump (9 Jun), and it meanders in the Gulf Stream (29 Jun–29 Jul). After leaving the stream east of 50°W, it exhibits eddy motion (30 Aug) and a slow drift to the south/west before its death 13 months later in Sep 1992. (b) These SOFAR float trajectories, launched by Tom Rossby as part of the POLYMODE Local Dynamics Experiment at a depth of 700 m in Jun 1978, are an early example of what a flow near a saddle point would look like. The position of the floats is given every day, with an arrow indicating their initial displacement.

the population performance in areas of relatively low average irradiance.

Spatial patterns in simulated phytoplankton distribution, induced by spatial inhomogeneities in the nutrient distribution, were analyzed by Lopez et al. (2001). The methodology is based on coupled discrete-time dynamical systems, which describe reaction or population dynamics and advection in the Lagrangian framework, applied to a model of logistic population dynamics in the presence of a localized source of nutrients and chaotic advection. Spatial structures with fractal, filament-like features are seen to appear in the phytoplankton field and have scales similar to that of the nutrient patch. An analogy with the random map model suggests that this behavior may originate with a change in the value of the reaction Lyapunov exponent relative to the spatial scale of the nutrient field.

Bracco et al. (2000c) point out that in situ observations contain a much larger number of plankton species than predicted by the competitive exclusion principle, which limits the number of species by the number of resources, the so-called paradox of the plankton problem. Solutions obtained by coupling a stochastic particle model (either a random walk or random flight) and competitive plankton models to simulations of barotropic turbulence show that less-fit plankton can be protected

from competition while trapped in vortices. These transport barriers allow the coexistence of more competitive species than predicted by the competitive exclusion principle (Bracco et al. 2000c).

4. Model–data comparisons and Lagrangian simulations

The number of investigations comparing results from Lagrangian data to results of different general and regional circulation models is increasing. Along with the traditional goal of such studies, namely the validation and improvement of the models, model results can be used to study properties of Lagrangian statistics and to gain insight into the relationships between Eulerian and Lagrangian velocity statistics. In addition to these more traditional applications, results from studies directed at a true Lagrangian utilization of numerical results, that is, the tracing of water masses and of particle and biogeochemical property exchange in the framework of realistic simulations of three-dimensional coastal and ocean circulation, are now approaching a more mature science.

A comparison has been performed between simulated mixed layer drifters from the Miami Isopycnal Coordinate Ocean Model (MICOM) and the near-surface drifters archived at the Atlantic Oceanographic and Meterological Laboratory (AOML) for the North and tropical Atlantic Ocean. MICOM was forced by climatological winds for 20 yr after Levitus initialization and was configured with 16 layers and a horizontal resolution of 1/12°. Two years after launch, the simulated particle density exhibited the well-known Ekman convergences and divergences. Pseudo-Eulerian mean velocity fields calculated from model trajectories and from in situ drifters, in general, showed good agreement. Problem areas were near the boundary of the model domain and near strong currents, due to the model placing the Gulf Stream, for example, a little too far north. The Lagrangian integral timescales were overestimated in the model by a factor of 2. This is presumably due to using relatively smooth climatological winds to force the model (Garraffo et al. 2001b).

Float–model comparisons have also been performed using the North Atlantic World Ocean Circulation Experiment surface drifters and simulated trajectories from both 0.1° and 0.28° horizontal resolution 40 vertical level North Atlantic configurations of the Los Alamos National Laboratory Parallel Ocean Program (POP) model, forced with 1993–97 Navy Operational Global Atmospheric Prediction System (NOGAPS) daily winds. The mean pseudo-Eulerian velocity statistics and estimates of the Lagrangian integral timescales from the simulation with 0.1° horizontal resolution were closer to in situ estimates than were those from the 0.28° simulation. The coarser-resolution simulation tended to overestimate the integral timescales (McClean et al. 2002).

A problem by which both of these model–data comparisons were hampered is the lack of in situ data, especially in the tropical Atlantic. Garraffo et al. (2001a) used the same MICOM surface velocity data as Garraffo et al. (2001b) and showed that the largest error source in calculating mean Eulerian velocity fields from Lagrangian data is sampling error. Bias errors (see Davis 1991) are also significant, due mostly to preferential sampling in divergent regions. Sampling error is a function of the finite data size and the variability associated with the unresolved flow scales. It will take a large number of in situ data to produce global maps of the climatological mean circulation because of the energetic and broad spectrum of sub- and mesoscale motions.

Garfield et al. (2001) compared simulated drifter trajectories from 0.28° horizontal resolution POP model simulations and 38 isobaric RAFOS floats in and near the California Undercurrent. Both in situ and simulated trajectories show the poleward-flowing California Undercurrent, a weak flow west of the undercurrent, and a strong westward-propagating eddy field that enhances the mixing between near-coastal water and the deep ocean. The model underestimated the mean flow and eddy kinetic energy level in this area, presumably because of coarse resolution.

Simulated trajectories from a two-dimensional shallow-water model and trajectories from visualized particles in the 14-m-diameter ''Coriolis'' rotating tank of the Laboratoire des Ecoulements Geophysiques et Industriels–Institut de Mecanique de Grenoble (LEGI–IMG) located at Grenoble, France, were compared. Experiments were conducted over a range of water depths, rotation rates, and spacing and speed of the grid used for stirring the fluid. The flow in these experiments, which span a range of (initial) Rossby numbers between 0.3 and 4.6 and Reynolds numbers between 10^3 and 10^4, is dominated by coherent vortices that trap fluid particles and are impermeable to inward particle fluxes. There was good agreement between the statistical properties of the numerical and visualized trajectories (Longhetto et al. 2001, manuscript submitted to *Nuovo Cimento C*).

Rolinski analyzed the results of a three-dimensional Lagrangian model (see Rolinski and Suendermann 2001a) for the transport, deposition, and resuspension of suspended particulate material (SPM), applied to the Elbe River in Germany. She compared different approaches for estimating the residual Lagrangian velocity from the baroclinic velocity field and used these residual velocities to study why SPM accumulates in freshwater regions in the estuary. Transport by coherent eddies is a dominant physical mechanism. She also discussed coupling this Lagrangian model to a finite-element model of the Venice lagoon (Rolinski and Suendermann 2001b). Difficulties include conversion of current fields from a finite-element circulation model onto a Lagrangian model that uses finite differences in a domain where wet/dry boundaries change rapidly. Special care must

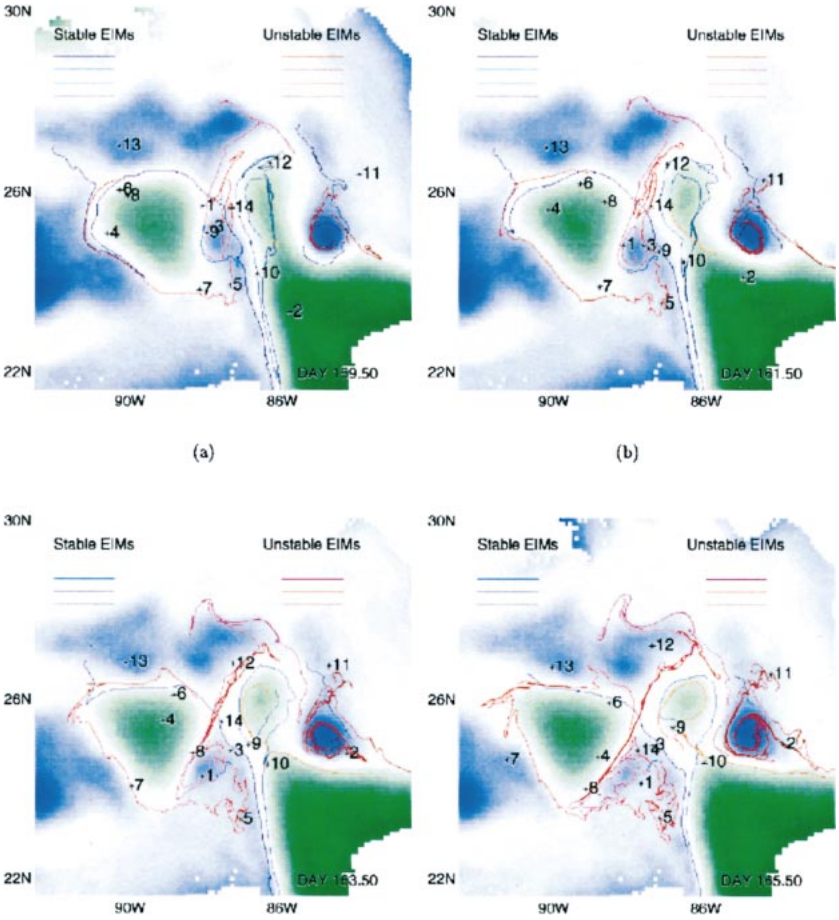

FIG. 2. Effective invariant manifolds (EIMs) in the eastern Gulf of Mexico during Jun 1998. The manifolds are computed from the 50-m horizontal velocity fields of a University of Colorado POM simulation, which assimilates satellite-derived temperature and height data, and are superimposed on the model height anomaly (green indicates positive and blue negative). The unstable EIMs (which grow in time) and the stable EIMs (which shrink in time) form the Lagrangian boundaries of coherent structures in the Eulerian velocity field. In the eastern Gulf, these structures are two anticyclones, two cyclones, and the Loop Current (LC). Positions of 14 drifters, deployed by Horizon Marine for Climatology and Simulation of Eddies, and then drogued at 50 m, are indicated by an asterisk (*). The data are shown every two days. (a) A small cyclone is between a northward meander in the LC to the east and an LC ring (LCR) to the west. A stationary Tortugas cyclone is to the east of the meander neck. The meander neck is forming another LCR. (b) The small cyclone travels south and begins to cleave the eastern edge of the large LCR. The meander neck narrows and recirculation begins in the new ring. (c) The small cyclone cleaves about 15% of the LCR. The separation of the meander into a new ring is more pronounced as the Lagrangian boundaries form. (d) The small cyclone and the cleaved portion of the LCR merge. Interesting drifter pairs are 6,8; 5,7; and 2,10. Drifters 6 and 8 are near each other in (a) and (b), but in (c) and (d) drifter 8 follows the eastern boundary of the LCR, while drifter 6 stalls near the stagnation point. Drifters 5 and 7 are near each other in (a), but in (b) drifter 5 is caught in the cleaved portion of the LCR, while drifter 7 remains in the main portion. Drifters 2 and 10 in (a) are on either side of the western boundary of the LC. Drifter 2, inside the LC, heads for the Tortugas cyclone (b) and just misses the northern LC boundary that is forming as the meander pinches (c). Drifter 10 heads toward the stagnation point (b), (c) and does not cross the northern LC boundary (d).

be used to set up volume-conserving equivalent elements based on complicated bathymetry and the amount of ''wet'' versus ''dry'' areas. It is important to conserve volume to reduce accumulation errors in the smallest grid volumes.

SPM simulations for the Thermaikos Gulf in Greece were compared by C. Koutitas (2000, personal communication) as a function of different assumptions for vertical particle motion. Daily average velocities from a Princeton Ocean Model (POM) simulation were used to advect particles; vertical movement was controlled by the local vertical velocity and the particle settling

velocity; turbulent diffusion was modeled as a Brownian process; and SPM processes such as resuspension, settling, and flocculation were also included in the model. Thirty thousand particles were tracked, and their average settling rate was 0.5–1.0 mm yr^{-1}. SPM processes lead to particles sinking at faster rates than those predicted by using just the local vertical velocities from the model.

Tracing the Water Masses (TRACMASS) is an offline code used to track water parcels that was applied to the output of a numerical simulation of the Mediterranean Sea. TRACMASS is fast, accurate, and able to track particles in three dimensions. For example, 100 000 parcels were launched at the Strait of Gibraltar at 50-m depth and tracked for hundreds of years. The mean arrival time for these particles was then calculated and mapped for the entire Mediterranean Sea. On timescales of a year, particles were advected along the North African coast. On timescales of decades, particles reached the eastern Mediterranean and filled out the basin. Particles reach the Adriatic Sea and northern Ionian basin on timescales of a hundred years, presumably due to the production of Levantine water that leads to relatively younger water sinking and changing its flow direction (V. Rupolo 2000, personal communication).

5. Applications of stochastic models

Stochastic models are used to study particle statistics in the ocean. In particular, non-Gaussian properties seen in the probability density functions (PDFs) of Lagrangian velocities can be modeled using stochastic models with a small number of parameters. The effects of non-Gaussian properties on model structure and dispersion properties are now being investigated. In general, stochastic models for Lagrangian particle trajectories in the ocean perform best at intermediate temporal lags. At small temporal lags, flow statistics are highly dependent on the flow conditions at the initial launch location, while at large temporal lags, boundary effects and the effects of potential vorticity constraints become dominant. Ironically, theoretical models for Lagrangian flow statistics are most easily derived for short times and for long times after launch.

Thompson (1986) formulated a random flight model for particle dispersion that is based on an Autoregressive model of order one, AR(1) (equivalently known as a Markov process), for turbulent velocities. The Markov random flight model differs from the random walk model by including a correlated velocity component that, in most applications, models the turbulent mesoscale. Thompson (1987) showed that the Lagrangian PDF for one-particle velocity statistics is related to the Eulerian PDF for the fluid velocity, since they both satisfy the same Fokker–Planck equation. Consequently, models of the Eulerian velocity PDFs are directly applicable to models of turbulent dispersion (e.g., Maurizi and Tampieri 1999).

The use of this model and parameter estimation for oceanic data is reviewed by Griffa (1996). The model has been used successfully in a number of applications such as prediction of Lagrangian motion (Falco et al. 2000) and modeling of dispersion in near-surface drifting buoys (Bauer et al. 1998), but in all of these studies the limitations of this model are clearly seen. The AR(2) and AR(3) models are now being evaluated by Berloff and McWilliams (2002), Berloff et al. (2002), and Pasquero et al. (2001). AR(2) models are needed when there is a strong looping motion or wave motion seen in particle trajectories. AR(3) models are needed when the velocity field has long-time memory that can result from being trapped in a vortex. It is usually assumed that the velocity components are independent, and each is of the form

$$dx = [U(x, y, t) + u(x, y, t)]dt$$

$$du = \frac{-u}{T_L}dt + \left(\frac{\sigma^2}{T_L}\right)^{1/2} d\eta,$$

where U is the mean flow, u is the turbulent velocity component modeled as an AR(1) process, σ^2 is the variance of the AR(1) (or Markov) process, T_L is the Lagrangian integral timescale [$T_L = \int_0^\infty C(\tau)\, d\tau$], and $d\eta$ is a white noise process. The velocity autocovariance function, $C(\tau)$, exponentially decays to zero with $C(2T_L) \approx 0$. Particle dispersion initially grows quadratically with time and then asymptotes to a linear function of time. The AR(1) model generalizes to an AR(2) model by also assuming that the particle acceleration a can be modeled as a Markov process with an integral timescale of T_a,

$$dx = [U(x, y, t) + u(x, y, t)]dt$$

$$du = a\,dt$$

$$da = -\left(1 + \frac{T_a}{T_L}a\right)\frac{dt}{T_a} - \frac{u}{T_L T_a}dt + \left[\frac{\sigma^2}{T_a}\left(1 + \frac{T_a}{T_L}\right)\right]^{1/2} d\eta.$$

The Lagrangian velocity autocorrelation function has two timescales, and, if $T_a > T_L$, the correlation can become negative. Note $\langle d\eta \cdot d\eta \rangle = 2dt$.

If the PDF of Lagrangian velocities was truly multivariate Gaussian and homogeneous in the ocean, then theoretical estimates of dispersion statistics would be exact, and we could derive, for example, a set of equations for an extended Kalman filter for assimilation of data into ocean circulation models that would be closed. However, at best, ocean statistics are only approximately Gaussian, and they are most definitely heterogeneous in space and nonstationary in time. Calculated PDFs, from in situ float data or from simulated trajectories from large eddy simulations of geostrophic turbulence and ocean circulation models, differ the most from a true Gaussian distribution in the tails of their distributions. Put simply, turbulent ocean flow is approximately Gaussian with more extreme values. Numerical and ex-

perimental results illustrating non-Gaussian PDFs are now performed at higher resolutions because of the ever-increasing computational power that is becoming available to researchers at lower and lower cost. In particular, Maurizi and Lorenzani (2000) analyzed experimental data from wall and shear-generated turbulence and suggested that the kurtosis K of the Eulerian velocity PDF is related to the skewness S by $K = c(S^2 + 1)$, where c is estimated to be in the range of 2.3–2.5.

It is now well known that coherent vortices can introduce far-field correlations that cannot be modeled using Gaussian statistics (McWilliams 1984; Weiss and McWilliams 1993; Bracco et al. 2000a,b). PPB investigated the behavior of an AR(1) stochastic particle model and a two-component stochastic model in a numerical simulation of forced barotropic turbulence on a doubly periodic 512×512 grid. The two-component model decomposes the velocity field into a background and a vortex component, and each component is modeled as an AR(1) process. This model is further improved by incorporating non-Gaussian behavior into the AR(1) model for the vortex component by allowing the AR coefficient to be a nonlinear function of the background velocity. PPB show that the dispersion statistics derived using an AR(1) model can be in error by as much as 25%, mostly at intermediate lags, and that exit times are underestimated and are a strong function of higher-order moments. Their nonlinear stochastic model significantly improved the exit time estimates.

Material spreading and mixing by oceanic mesoscale eddies are analyzed in an idealized, numerical model of the wind-driven, midlatitude oceanic circulation (Berloff et al. 2002). The analyses are based on ensembles of Lagrangian particle trajectories. It is shown that tracer transport by mesoscale eddies differs in many ways from the commonly used model of homogeneous, isotropic eddy diffusion. The results suggest reconsideration of the traditional diffusion approach. A hierarchy of inhomogeneous, nonstationary stochastic models of material transport is formulated, and its properties are described by Berloff and McWilliams (2002). The transport models from the hierarchy sequence provide progressively more skillful simulations of the subgrid-scale transport by mesoscale eddies, which are typically not resolved in coarse-grid representations of the ocean circulation. Performance of the models is evaluated by (a) estimating their parameters from Eulerian and Lagrangian statistics of a fluid-dynamic reference solution, (b) solving for the transport, and (c) comparing the stochastic and direct fluid-dynamic transports.

Numerical results from these and other simulations and some observational evidence suggest that single-particle dispersion statistics are not linear in time at intermediate lags, as suggested by Taylor (1921). Subdiffusion results when particles are trapped by vortices and planetary waves, while superdiffusion can be found in western boundary regions. Subdiffusion leads to negative lobes in the velocity autocorrelation function, while superdiffusion leads to enhanced positive correlations. AR(2) models are a big improvement over AR(1) models, especially in deep layers that exhibit ''oscillatory'' velocity correlation functions. AR(3) stochastic models are needed for superdiffusive flows when mean advection dominates.

G. Buffoni (2000, personal communication) analyzed the dispersion properties of particles in a semienclosed basin by assuming that there are no particle interactions and that the probability of finding a particle in the basin is the same for all particles. Under these assumptions, the number of particles in the basin at any instant of time has a binomial distribution. Even though these assumptions could easily be questioned, numerical simulations with various flows are able to reproduce the theoretical estimates of mean residence times and their variance.

6. Nonlinear dynamics and dynamical system theory

There is a one-to-one correspondence between the phase space of dynamical system analysis and the physical space of a two-dimensional fluid. This correspondence can be exploited to relate mathematical phenomena such as the Kolmogorov–Arnold–Moser (KAM) tori, chaos, and invariant manifolds to physical phenomena such as fluid transport barriers, efficient stirring, and mixing of fluids and the geometry of particle trajectories, respectively (Babiano et al. 1994; Wiggins 1992). Recent techniques have focused on identifying hyperbolic stagnation points, defined by the intersection of a stable manifold (fluid particles are attracted toward the hyperbolic point) and unstable manifolds (particles are repelled away from the hyperbolic point) from a nonlinear analysis of the critical points of a velocity field. Lobe dynamics (Malhotra and Wiggins 1998) identify the most important intersection of stable and unstable manifolds, basically moving saddle points known as hyperbolic trajectories that divide the flow into distinct regimes. The rate of fluid mixing can be calculated as a function of the area of the lobes.

It is extremely challenging to detect hyperbolic trajectories in large, model-generated velocity fields or oceanographic data that are, in general, finite in time, aperiodic, noisy, three-dimensional in space, gappy, and may have open boundaries. Methods are being developed to overcome each of these difficulties (Wiggins 1992; Coulliette and Wiggins 2000; Malhotra and Wiggins 1998; Haller and Poje 1998; Haller 2000; Miller et al. 1997). Efficient methods for finding the *distinguished hyperbolic trajectories* for large, time-dependent sets are discussed in Ide et al. (2001), F. Lekein (2000, personal communication), and Kuznetsov et al. (2001, manuscript submitted to *J. Mar. Res.*, hereafter KUZ). These methods define the distinguished hyperbolic trajectories (DHTs) (or equivalent) based on frozen-time/instantaneous stagnation points and zero ve-

locity curves. DHTs divide the flow field into different regimes with similar properties, such as residence time of particles.

Ide et al. (2002) applied her analysis to velocity fields from a classic, wind-driven double-gyre ocean model simulation. The Eulerian transport is defined as the net amount of fluid particles and properties that migrate from one region to another across a stationary boundary over a time interval. Ide defined the stationary boundary by a reference streamline determined by a nonlinear analysis and defined as the DHTs. Efficient algorithms for identifying DHTs in large, model-generated datasets are detailed in Ide et al. (2002).

F. Lekien (2000, personal communication) analyzed the intergyre exchange from a three-layer quasigeostrophic (QG) double-gyre model simulation in a (2000 km)^2 domain. He showed that DHTs and stagnation points can be as far apart as 300 km. This justifies the need for an accurate method to compute those DHTs, even though the associated computational load is considerable. The intergyre transport was shown to be a function of the lobes that define the intersection of the stable and unstable manifold of the DHTs.

KUZ analyzed Gulf of Mexico simulations from the POM model. Effective invariant manifolds (EIMs) can be computed from ''noisy'' model fields and used to identify flow structure. EIMs are distinct regions in the fluid flow with similar properties. This analysis quantified the exchange of water between an anticyclonic Loop Current warm-core ring and a small cyclonic eddy, and provided a detailed history of ring formation. The analysis showed that cyclonic rings have enhanced mixing regions along their boundary and that the larger anticyclonic rings were relatively isolated (see Fig. 2).

Dispersion and mixing can also be studied using tools from nonlinear dynamical systems theory. A. Vulpiani (2000, personal communication) pointed out that asymptotic estimates of tracer dispersion are not possible in small domains where the dominant Eulerian length scale is not much smaller than domain size because of boundary effects. Vulpiani used finite-scale Lyapunov exponents (FSLEs) to estimate that one-particle dispersion can grow as t^3 in simple chaotic flows. FSLEs, $L(R)$, are a generalization of Lyapunov exponents (LEs), L, that are a function of the separation distance between particles, R, and that are used to quantify dispersion. In the limit of R approaching zero, $L(R) = L$. When L is positive, the fluid undergoes chaotic mixing. When R is less than the domain size, Rmax, $L(R)$ scales as D/R^2 (velocity variance approximately equals $4Dt$ at time t), and for R approximately Rmax, $L(R)$ scales as (Rmax $- R$)/R, where the coefficient is the inverse of the relaxation time to uniform particle distribution.

FSLEs were used to analyze the dispersion of simulated trajectories in an ocean general circulation model of the Mediterranean Sea. Spatial maps of FSLEs indicated regions with strong turbulent mixing, as well as regions with weak mixing. Relative dispersion was dominated by mean shear effects up to gyre scales and by mesoscale chaotic advection. FSLEs were also used to analyze tracked Lagrangian particles from an essentially two-dimensional convection experiment that exhibited strong chaotic motion at a large Rayleigh number [Ra $\propto O(10^8)$]. The Lagrangian motion was found to be chaotic with a Lyapunov exponent that scales with the Rayleigh number as Ra$^{1/2}$ (Boffetta et al. 1999, 2000).

Abel et al. (2002) used Bower's (1991) analytical streamfunction to model the mean Gulf Stream. Turbulent Lagrangian trajectories of passively advected particles were then calculated. In order to analyze particle tracks, the Gulf Stream region was divided into three areas (states): a southern gyre, a jet, and a northern gyre. A symbolic sequence was formed, using the exit time formalism (Abel et al. 2000) that brackets the time spent in each state, from the sequence of the particles passing through the states. The symbolic sequence was filtered to separate the two inherent timescales—slow and fast—of the system. A random traveler description of the particle tracks was derived for each of the filtered sequences of exit times and states. The sequence is shown to be of Markovian order one and constitutes a hierarchy of Markovian processes, one level for each of the two timescales. By means of entropic analysis, it is evident that this hierarchical model with a first-order Markovian model for each timescale is sufficient to describe the dynamics of the advected particle.

7. Lagrangian predictability and assimilation of Lagrangian data

Lagrangian predictability is of great importance for practical applications such as search and rescue operations and dispersal of pollutants. The prediction of Lagrangian trajectories is an extremely difficult problem because of the inherent chaotic nature of nonlinear advection and because of our limited knowledge of the ocean velocity field. Various approaches to this problem are now being formulated. Recent simulations by Özgökmen et al. (2000, 2001) and Castellari et al. (2001) showed that accurate predictions, 1-week forecast errors $<$15 km, are possible if enough contemporary Lagrangian data are available for assimilation. Predictive skills increase using a simplified Kalman filter that assimilates Lagrangian data for Lagrangian prediction relative to estimates based on the movement of the center of mass of the data cluster or integrating climatological velocity fields. A normalized data density DD was defined as nd/md^2, where md is the mean diameter of the floats in the cluster and nd is the number of floats. For DD > 1 drifter per degrees squared, only the Kalman-based filter assimilating Lagrangian data produced accurate estimates of near-surface buoy trajectories in the tropical Pacific.

A new improved Kalman filtering algorithm for Lagrangian prediction, based on a consistent stochastic model for multiparticle Lagrangian motion in the upper

ocean, was formulated by Piterbarg (2001b) and is now being evaluated for the above-mentioned buoys. The dependence of the Lyapunov exponent/predictability on parameters such as the Lagrangian correlation time and the Eulerian velocity–space correlation radius has been investigated (Piterbarg 2001a). A general relation between Lagrangian stochastic models and Eulerian equations with stochastic forcing can be formulated and used, for example, for assimilating Lagrangian data into ocean circulation models written in the Eulerian form.

The prediction of constant level ''balloon trajectories'' in the atmosphere can be obtained by using an estimate of the Eulerian winds from the European Centre for Medium-Range Weather Forecasts (ECMWF) and a particle model with a simple linear Rayleigh friction that is proportional to the velocity (Dvorkin et al. 2001). This approach was applied to balloons launched in Ecuador in the summer of 1998 by the French EQUATEURE experiment. Best fits to observed EQUATEURE trajectories yielded a 1-day relaxation time for the Rayleigh friction coefficient and the finding that 85% of the position variability can be explained by advection by the winds. The 15% contribution from the particle model reduced the prediction error of balloon positions by 50%. Preliminary results for this technique when applied to near-surface buoys in the tropical Pacific indicate a significant improvement, relative to advection by the climatological mean velocity field, in predicting Lagrangian trajectories.

Another outstanding research problem is how to best assimilate Lagrangian data into numerical circulation models. Lagrangian data are usually assimilated as moving Eulerian measurements. The Lagrangian nature of the data is usually not accounted for in data assimilation schemes. Work in progress by Chin uses results from twin experiments in which Lagrangian data were assimilated into a four-layer, 20-km horizontal resolution wind-driven double-gyre experiment using MICOM, a reduced-order information filter (Chin et al. 1999), and the assumption of treating the Lagrangian data as moving Eulerian data. Information from the velocity field was shown to improve predictions of both surface velocity and sea surface height. As a first step toward optimizing the Lagrangian information content of drifter data in data assimilation, trajectory position information was assimilated using the ''snake'' algorithm to minimize the distance between simulated float trajectories and ''data'' (float trajectories from the twin experiment) by correcting the model velocity field. The shape and strength of circulation features were improved.

Toner et al. (2001) presented results from model simulations of the Gulf of Mexico using the POM model and assimilating Lagrangian data by constraining the GOFs to match the Lagrangian velocities from drifters drogued at 50 m. The constrained GOF-based reconstructed Eulerian velocity field improved forecasts of drifter trajectories by an order of magnitude in a 450-km^2 subdomain of the model with a Loop Current warm-core ring.

The development of an ocean circulation model formulated in Lagrangian coordinates would lead to optimal assimilation of Lagrangian information contained in float trajectories. When assimilating Lagrangian data into regional primitive equation models, Lagrangian coordinates offer two distinct advantages because the float trajectories are the dependent state variables of the model. These advantages are that 1) no model–data interpolation is needed and 2) simulations with open domains have well-posed forward and backward problems (Bennett and Chua 1999; Mead and Bennett 2001). The primary disadvantages are the highly nonlinear pressure gradient term and the fact that viscosity can introduce spurious boundary layers. This shallow-water model with Lagrangian coordinates was able to reproduce the eddy field, compared to a similarly forced traditional Eulerian circulation model in a doubly periodic domain for numerical simulations lasting a few months.

8. Concluding remarks

Important and complex research issues, discussed by working groups at the LAPCOD meeting, are the following:

1) What improvements in modeling, analysis, float design, and sampling are needed for coastal and biological applications?
2) How can the exchange of information between theoreticians and those collecting Lagrangian data be optimized? For example, what data are needed for better turbulence closure schemes, and what do numerical simulations of turbulence/stochastic models tell us about designing optimal Lagrangian-based sampling schemes for the ocean and coastal waters?
3) How can the information from Argo profiling floats be optimized for improving our understanding of ocean circulation and dynamics and for assimilation into ocean circulation models? How can we optimize the Lagrangian information content of floats for data assimilation?

More realistic models, new instrument and sensor designs, and high-resolution mapping of ''index species'' are especially needed to improve our understanding of the coastal–deep water exchange processes. This will be especially challenging, due to the small space scales and rapid timescales of both oceanic and atmospheric velocity fields, species patchiness, and the fuzziness/complicated geometry of the coastal–deep water boundary as seen in ocean color and thermal observations. Achieving this goal will require a multidisciplinary effort to improve atmospheric forcing fields for nested coastal models, to provide high-resolution maps of bottom bathymetry, to launch smart ''intelligent'' floats with a suite of multispectral and chemical sensors, and to place arrays of acoustic trackers to estimate biomass

on all trophic levels from zooplankton to tuna. Smarter floats with better water-following properties will be needed to sample shelf exchange processes and shorelines with complicated geometries.

The primary recommendation for sampling design was to launch floats in clusters. More specifically, three to four floats seemed to be a good compromise between finite resources, regional coverage, and information on multiparticle statistics. On short timescales, this Lagrangian data can be used to estimate the parameters of one- and two-particle dispersion models, to estimate velocity gradients for dynamical balance (e.g., momentum, potential vorticity) studies, and to constrain the velocity field of numerical simulations via data assimilation. Lagrangian data combined with high-resolution surface velocity maps from radar imaging techniques enables one to test various parameterization schemes for vorticity dissipation.

Model–data comparisons of the near-surface velocity field have been hampered by lack of data in divergent regions such as the equatorial Pacific and the upwelling zones off West Africa. To increase the amount of data in divergent regions would require a preferential deployment of floats in these regions to ensure equal sampling density. Possible biases in dispersion statistics due to preferential deployment should be studied. Climatological datasets for model–data comparisons are available (e.g., at www.aoml.noaa.gov/phod/dac/dacdata.html and wfdac.whoi.edu). However, data for real-time forecasting of sea surface velocity is not readily available but should be in the near future.

The optimization of information from the planned large array of profiling floats in the ocean is an extremely timely and daunting task. Profiling floats are providing a wealth of hydrographic data, including data in historically data-void regions of the World Ocean. These data will definitely increase our confidence in the time-averaged dynamic height maps and resulting relative velocity fields, and it will constrain the thermohaline variables in numerical models. This constraint is important, given our sparse and noisy estimates of surface fluxes of heat and salt. However, the position and velocity data at the floats' deep travel depth of 1000–2000 m from this large dataset will require new algorithms for real-time operational data assimilation. Except in strong current regimes, the present sampling of two positions every 7 to 14 days may lead to velocity estimates dominated by energetic eddies, since the present sampling rate for position data for profiling floats is of the same order as the eddy timescales. The use of these velocity estimates in present operational data assimilation methods that treat Lagrangian data as moving Eulerian measurements may lead to biases, unless new techniques that take into account both the integrating aspect of Lagrangian measurements and the highly nonlinear relationship between Eulerian and Lagrangian velocities are developed, or a truly Lagrangian-based ocean circulation model is used. Regions of strong vertical velocity shears can introduce errors as large as 50% in estimating the deep absolute reference velocity. It is recommended that the next generation of profiling floats should be tracked so that position and velocity data can be generated over the entire 7–14-day period. Of course, such tracking will require greater resources that may reduce the number of floats or their geographical extent, so extensive numerical simulations should be conducted to optimize limited resources. The planned large array of profiling floats should be launched in clusters since they will disperse to the planned horizontal resolution of one float per 5° within a month or so after launch, and clusters would provide a wealth of data for stochastic models and Lagrangian predictability studies.

Acknowledgments. The LAPCOD 2000 meeting and the writing of this review paper were made possible by Grants N00014-99-1-0049 and N00014-00-1-1071 from the Office of Naval Research, which deserves the greatest gratitude. The PIs gratefully acknowledge the technical skills of Ed Ryan as the webmaster of our LAPCOD site, http://www.rsmas.miami.edu/LAPCOD/. The local team of Angela Landolfi, PierPaolo Falco, and Daniela Cianelli did a superb job of providing network access, running a wide variety of laptops and A/V equipment. Liz Williams provided the data for Fig. 1, and Michael Toner provided Fig. 2. Joanna Gyory and Linda Smith provided editorial assistance. The authors greatly appreciate the input of Mike Clancy on an earlier version of this paper.

REFERENCES

Abel, M., L. Biferale, M. Cencini, M. Falcioni, D. Vergni, and A. Vulpiani, 2000: Exit-time approach to *ϵ-entropy*. *Phys. Rev. Lett.,* **84,** 6002–6005.

——, K. H. Andersen, and G. Lacorata, 2002: Hierarchical Markovian modelling of multi-time scale systems. *Physica D,* in press.

Babiano, A., A. Provenzale, and A. Vulpiani, Eds.,1994: Chaotic advection, tracer dynamics, and turbulent dispersion. Proceedings of the NATO Advanced Research Workshop and EGS Tropical Workshop on Chaotic Advection, Conference Centre Sereno di Gavo, Italy, 24–28 May 1993. *Physica D,* **76,** 1–329.

Bauer, S., M. Swenson, A. Griffa, A. J. Mariano, and K. Owens, 1998: Eddy–mean flow decomposition and eddy-diffusivity estimates in the tropical Pacific Ocean. *J. Geophys. Res.,* **103** (C13), 30 855–30 871.

Bennett, A. F., and B. S. Chua, 1999: Open boundary conditions for Lagrangian geophysical fluid dynamics. *J. Comput. Phys.,* **153,** 418–436.

Berloff, P., and J. McWilliams, 2002: Material transport in oceanic gyres. Part II: Hierarchy of stochastic models. *J. Phys. Oceanogr.,* **32,** 797–830.

——, ——, and A. Bracco, 2002: Material transport in oceanic gyres. Part I: Phenomenology. *J. Phys. Oceanogr.*, **32,** 764–796.

Bezerra, M. O., M. Diez, C. Medeiros, A. Rodriguez, E. Bahia, A. Sanchez-Arcilla, and J. M. Redondo, 1998: Study on the influence of waves on coastal diffusion using image analysis. *Appl. Sci. Res.*, **59,** 127–142.

Boffetta, G., M. Cencini, S. Espa, and G. Querzoli, 1999: Experimental evidence of chaotic advection in a convective flow. *Europhys. Lett.,* **48,** 629–633.

——, ——, ——, and ——, 2000: Chaotic advection and relative

dispersion in an experimental convective flow. *Amer. Inst. Phys.*, **12,** 3160–3167.
Bower, A. S., 1991: A simple kinematic mechanism for mixing fluid parcels across a meandering jet. *J. Phys. Oceanogr.*, **21,** 173–180.
——, N. Serra, and I. Ambar, 2002: Spreading of Mediterranean Water around the Iberian Peninsula. *J. Geophys. Res.*, in press.
Bracco, A., J. LaCasce, C. Pasquero, and A. Provenzale, 2000a: The velocity distribution of barotropic turbulence. *Amer. Inst. Phys.*, **12,** 2478–2488.
——, J. C. McWilliams, G. Murante, A. Provenzale, and J. B. Weiss, 2000b: Revisiting freely decaying two-dimensional turbulence at millennial resolution. *Amer. Inst. Phys.*, **12,** 2931–2941.
——, A. Provenzale, and I. Scheuring, 2000c: Mesoscale vortices and the paradox of the plankton. *Proc. Roy. Soc. London*, **B267,** 1795–1800.
Castellari, S., A. Griffa, T. M. Özgökmen, and P.-M. Poulain, 2001: Prediction of particle trajectories in the Adriatic Sea using Lagrangian data assimilation. *J. Mar. Syst.*, **29,** 33–50.
Chin, T. M., A. J. Mariano, and E. P. Chassignet, 1999: Spatial regression and multi-scale approximations for sequential data assimilation in ocean models. *J. Geophys. Res.*, **104** (C4), 7991–8014.
Coulliette, C., and S. Wiggins, 2000: Intergyre transport in a wind-driven, quasigeostrophic double gyre: An application of lobe dynamics. *Nonlinear Proc. Geophys.*, **7,** 59–85.
Cowen, R. K., K. M. M. Lwiza, S. Sponaugle, C. B. Paris, and D. B. Olson, 2000: Connectivity of marine populations: Open or closed? *Science*, **287,** 857–859.
Davis, R. E., 1991: Observing the general circulation with floats. *Deep-Sea Res.*, **38,** S531–S571.
Dvorkin, Y., N. Paldor, and C. Basdevant, 2001: Reconstructing balloon trajectories in the tropical stratosphere with a hybrid model using analyzed fields. *Quart. J. Roy. Meteor. Soc.*, **127,** 975–988.
Falco, P., A. Griffa, P. M. Poulain, and E. Zambianchi, 2000: Transport properties in the Adriatic Sea as deduced from drifter data. *J. Phys. Oceanogr.*, **30,** 2055–2071.
Garfield, N., M. E. Maltrud, C. A. Collins, T. A. Rago, and R. G. Paquette, 2001: Lagrangian flow in the California Undercurrent, an observation and model comparison. *J. Mar. Syst.*, **29,** 201–220.
Garraffo, Z., A. Griffa, A. J. Mariano, and E. P. Chassignet, 2001a: Lagrangian data in a high resolution model simulation of the North Atlantic. II: On the pseudo-Eulerian averaging of Lagrangian data. *J. Mar. Syst.*, **29,** 177–200.
——, A. J. Mariano, A. Griffa, C. Veneziani, and E. P. Chassignet, 2001b: Lagrangian data in a high resolution model simulation of the North Atlantic. I: Comparison with in-situ drifter data. *J. Mar. Syst.*, **29,** 157–176.
Griffa, A., 1996: Applications of stochastic particle models to oceanographic problems. *Stochastic Modelling in Physical Oceanography*, R. J. Adler, P. Muller, and B. L. Rozovskii, Eds., Birkhauser, 114–140.
Haller, G., 2000: Finding finite-time invariant manifolds in two-dimensional velocity fields. *CHAOS*, **10,** 99–108.
——, and A. Poje, 1998: Finite time transport in aperiodic flows. *Physica D*, **119,** 352–380.
Hitchcock, G. L., W. L. Wiseman Jr., W. C. Boicourt, A. J. Mariano, N. Walker, T. Nelsen, and E. H. Ryan, 1997: Property fields in the effluent plume of the Mississippi River. *J. Mar. Syst.*, **12,** 109–126.
Ide, K., D. Small, and S. Wiggins, 2002: Distinguished hyperbolic trajectories in time dependent fluid flows: Analytical and computational approach for velocity fields defined as data sets. *Nonlinear Proc. Geophys.*, in press.
Lipphardt, B. L., A. D. Kirwan Jr., C. E. Grosch, J. K. Lewis, and J. D. Paduan, 2000: Blending HF radar and model velocities in Monterrey Bay through normal mode analysis. *J. Geophys. Res.*, **105,** 3425–3450.
Lopez, C., E. Hernandez Garcia, O. Piro, A. Vulpiani, and E. Zambianchi, 2001: Population dynamics advected by chaotic flows: A discrete-time map approach. *CHAOS*, **11,** 397–407.
Malhotra, N., and S. Wiggins, 1998: Geometric structures, lobe dynamics, and Lagrangian transport in flows with aperiodic time dependence, with applications to Rossby wave flow. *J. Nonlinear Sci.*, **8,** 401–456.
Mariano, A. J., and H. T. Rossby, 1989: The Lagrangian potential vorticity balance during POLYMODE. *J. Phys. Oceanogr.*, **19,** 927–939.
Maurizi, A., and F. Tampieri, 1999: Velocity probability density functions in Lagrangian dispersion models for inhomogeneous turbulence. *Atmos. Environ.*, **33,** 281–289.
——, and S. Lorenzani, 2000: On the influence of the Eulerian velocity PDF closure on the eddy diffusion coefficient. *Bound.-Layer Meteor.*, **95,** 427–436.
McClean, J. L., P.-M. Poulain, J. W. Pelton, and W. E. Maltrud, 2002: Eulerian and Lagrangian statistics from surface drifters and a high-resolution POP simulation in the North Atlantic. *J. Phys. Oceanogr.*, in press. [Also available online at http://po.gso.uri.edu/wbc/Mcclean/index.html]
McWilliams, J. C., 1984: The emergence of isolated coherent vortices in turbulent flow. *J. Fluid Mech.*, **146,** 21–43.
Mead, J. L., and A. F. Bennett, 2001: Towards regional assimilation of Lagrangian data: The Lagrangian form of the shallow-water model and its inverse. *J. Mar. Syst.*, **29,** 365–384.
Miller, P. D., C. K. R. T. J. Jones, A. Rogerson, and L. J. Pratt, 1997: Quantifying transport in numerically generated velocity fields. *Physica D*, **110,** 105–122.
Özgökmen, T. M., A. Griffa, A. J. Mariano, and L. I. Piterbarg, 2000: On the predictability of Lagrangian trajectories in the ocean. *J. Atmos. Oceanic Technol.*, **17,** 366–383.
——, L. I. Piterbarg, A. J. Mariano, and E. Ryan, 2001: Predictability of drifter trajectories in the tropical Pacific Ocean. *J. Phys. Oceanogr.*, **31,** 2691–2720.
Pasquero, C., A. Provenzale, and A. Babiano, 2001: Parameterization of dispersion in two-dimensional turbulence. *J. Fluid Mech.*, **439,** 279–303.
Peters, H., L. K. Shay, A. J. Mariano, and T. M. Cook, 2002: Current variability on a narrow shelf with large ambient vorticity. *J. Geophys. Res.*, in press.
Piterbarg, L. I., 2001a: The top Lyapunov exponent for a stochastic flow, modeling the upper ocean turbulence. *SIAM J. Appl. Math.*, **62,** 777–800.
——, 2001b: Short-term prediction of Lagrangian trajectories. *J. Atmos. Oceanic Technol.*, **18,** 1398–1410.
Polivina, J. J., P. Klieber, and D. R. Kobayashi, 1999: Application of TOPEX-POSEIDON satellite altimetry to simulate transport dynamics of larvae of spiny lobster, *Panilurus marginatus*, in the northwestern Hawaiian Islands, 1993–1996. *Fish. Bull.*, **97,** 132–143.
Poulain, P.-M., 1999: Drifter observations of surface circulation in the Adriatic Sea between December 1994 and March 1996. *J. Mar. Syst.*, **20,** 231–253.
——, 2001: Adriatic Sea surface circulation as derived from drifter data between 1990 and 1999. *J. Mar. Syst.*, **29,** 3–32.
Rolinski, S., and J. Suendermann, 2001a: Description of the suspended particulate matter phytobenthos reaction model. Tech. Rep. MAS3-CT97-0145 F-ECTS-REL-T043.
——, and ——, 2001b: Modelling the dynamics of suspended particulate matter and phytobenthos—Report on the application to Venice Lagoon. Tech. Rep. MAS3-CT97-0145 F-ECTS-REL-T049.
Rossby, H. T., S. C. Riser, and A. J. Mariano, 1983: The western North Atlantic—A Lagrangian viewpoint. *Eddies in Marine Science*, A. R. Robinson, Ed., Springer-Verlag, 66–91.
Sabatis, A., J. Salat, and M. P. Olivar, 2001: Advection of continental water as an export mechanism for anchovy, *Engraulis encrasicolus*, larvae. *An Interdisciplinary View of the Ocean*, J. L.

Pelegrm, I. Alonso, and J. Arstegui, Eds. *Sci. Mar.*, **65** (Suppl. 1), 77–87.

Shay, L. K., and Coauthors, 2000: A submesoscale vortex detected by very high resolution radar. *EOS*, **81**.

Taylor, G. I., 1921: Diffusion by continuous movements. *Proc. London Math. Soc.*, **20,** 196–212.

Thompson, D. J., 1986: A random walk model of dispersion in turbulent flows and its application to dispersion in a valley. *Quart. J. Roy. Meteor. Soc.*, **112,** 511–529.

——, 1987: Criteria for the selection of stochastic models of particle trajectories in turbulent flow. *J. Fluid Mech.*, **180,** 529–556.

Toner, M., A. D. Kirwan Jr., L. Kantha, and J. Choi, 2001: Can general circulation models be assessed and their output enhanced with drifter data? *J. Geophys. Res.*, **106,** 19 563–19 579.

Weis, J. B., and J. C. McWilliams, 1993: Temporal scaling behavior of decaying two-dimensional turbulence. *Phys. Fluids*, **A5,** 608–621.

Wiggins, S., 1992: *Chaotic Transport in Dynamical Systems*. Springer-Verlag, 301 pp.

Wilson, W. D., and K. D. Leaman, 2001: Transport pathways through the Caribbean: The tropical origins of the Gulf Stream. *J. Mar. Ed.*, **16,** 14–17.

Wolanski, E., P. Doherty, and J. Carleton, 1997: Directional swimming of fish larvae determines connectivity of fish populations on the Great Barrier Reef. *Naturwissenschaften*, **84** (6), 262–268.

Ye, J., and R. W. Garvine, 1998: A model study of estuary and shelf tidally driven circulation. *Cont. Shelf Res.*, **18,** 1125–1155.

Zhang, H. M., M. D. Prater, and T. Rossby, 2001: Isopycnal Lagrangian statistics from the North Atlantic Current RAFOS float observations. *J. Geophys. Res.*, **106** (C7), 13 817–13 836.